

A mixed-valence diacetate-bridged Mn^{II}–Mn^{III} complex incorporating a bridging phenolate ligand

Adailton J. Bortoluzzi, Ademir Neves,* Ricardo A. A. Couto and Rosely A. Peralta

Departamento de Química – UFSC, 88040-900 Florianópolis, SC, Brazil
Correspondence e-mail: adajb@qmc.ufsc.br

Received 26 July 2005

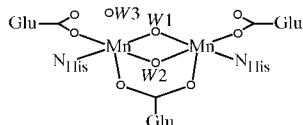
Accepted 30 November 2005

Online 14 January 2006

The synthesis and characterization of a new unsymmetrical dinucleating *N,O*-donor ligand, 2-[*N,N*-bis(2-pyridylmethyl)aminomethyl]-6-[*N*-(3,5-di-*tert*-butyl-2-oxidobenzyl)-*N*-(2-pyridylamino)aminomethyl]-4-methylphenol (H₂Ldtb), as well as the X-ray crystal structure of its corresponding mixed-valence diacetate-bridged manganese complex, di- μ -acetato- μ -{2-[*N,N*-bis(2-pyridylmethyl)aminomethyl]-6-[*N*-(3,5-di-*tert*-butyl-2-oxidobenzyl)-*N*-(2-pyridylamino)aminomethyl]-4-methylphenolato}dimanganese(II,III) tetraphenylborate, [Mn^{II}-Mn^{III}(C₄₂H₄₉N₅O₂)(C₂H₃O₂)₂](C₂₄H₂₀B), are reported. The complex may be regarded as an interesting structural model for the mixed-valence Mn^{II}–Mn^{III} state of manganese catalase.

Comment

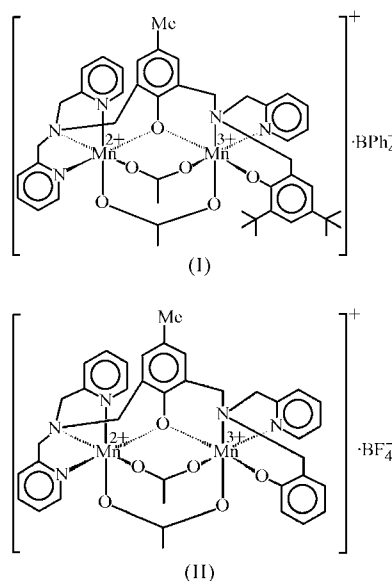
Catalases are enzymes responsible for hydrogen peroxide dismutation, according to the reaction 2H₂O₂ → O₂ + 2H₂O. The dimanganese catalase extracted from *Thermus thermophilus* was recently characterized by X-ray diffraction analysis, which confirmed the existence of a dinuclear manganese centre in the active site situated in a cavity rich in hydrophobic residues (see scheme) (Barynin *et al.*, 1997; Antonyuk *et al.*, 2000). The Mn^{II}–Mn distance is 3.18 Å in the reduced form (Mn₂^{II}) and 3.14 Å in the oxidized form (Mn₂^{III}). On the other hand, the mixed-valence Mn^{II}–Mn^{III} oxidation state is the least well characterized, and the *Lactobacillus plantarum* enzyme has not been shown to form a stable Mn^{II}–Mn^{III} form (Waldo *et al.*, 1995; Khangulov *et al.*, 1990). In fact, the design of biomimetic systems aiming to help in the understanding of



the mechanism of H₂O₂ disproportionation by manganese catalases has attracted many research groups (Wu *et al.*, 2004).

We report here the synthesis and X-ray structure of the title novel mixed-valence Mn^{II}–Mn^{III} complex, (I), containing the unsymmetrical dinucleating ligand Ldtb²⁻ {H₂Ldtb is 2-[*N,N*-bis(2-pyridylmethyl)aminomethyl]-6-[*N*-(3,5-di-*tert*-butyl-2-oxidobenzyl)-*N*-(2-pyridylmethylamino)amino]-4-methylphenol} and acetate bridges, as a further interesting structural model for mixed-valence Mn^{II}–Mn^{III} catalase.

The asymmetric unit of (I) consists of a discrete [Mn^{II}-Mn^{III}(Ldtb)(μ -OAc)₂]⁺ cation complex and a tetraphenylborate counter-ion. In the crystal structure, the packing arrangement is governed by electrostatic forces between ion pairs. The molecular structure of (I) (Fig. 1) shows that, in the dinuclear [Mn^{III}Mn^{II}(Ldtb)(μ -OAc)₂]⁺ unit, the Mn^{III} and Mn^{II} ions are bridged by phenolate atom O1 of the Ldtb²⁻ ligand and by two carboxylate groups of the acetate ligands. The charge distribution is the major contributor to the enhanced stability of the mixed-valence species, as observed by Dubois *et al.* (2003). Atoms N1, N22 and N32, from the tertiary amine and two pyridine groups (soft side), complete the octahedral coordination sphere of Mn1, typical of high-spin Mn^{II} (Karsten, Neves, Bortoluzzi, Stähle & Maichle-Mössmer, 2002). A comparison of the bond lengths around the six-coordinated Mn^{II} ion (Table 1; mean 2.201 Å) are in good agreement with those reported by Karsten, Neves, Bortoluzzi, Strähle & Maichle-Mössmer (2002) for the compound [Mn^{II}-Mn^{III}(bpbmp)(OAc)₂](BF₄), (II), where H₂bpbmp is the ligand {2-[*N,N*-bis(2-pyridylmethyl)aminomethyl]-6-[(2-hydroxybenzyl)(2-pyridylmethyl)]aminomethyl]-4-methylphenol, and by Karsten, Neves, Bortoluzzi, Lanznaster & Drago, (2002) in the compound [Mn^{II}Fe^{III}(bpbmp)(OAc)₂](ClO₄), (III).



The distances around Mn^{II} average 2.210 Å in (II) and 2.206 Å in (III), with the same N₃O₃ environment as (I). The distances from the pyridine N atom to Mn1 in (I) are quite similar [2.237 (3) and 2.262 (4) Å], while the distance of the N atom *trans* to the oxygen bridge is slightly longer, reflecting

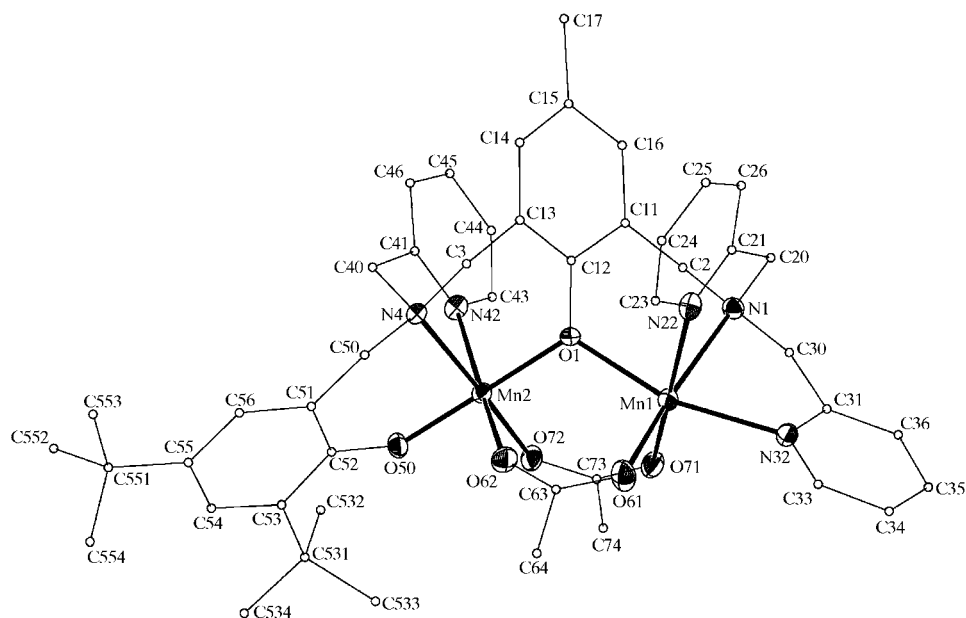


Figure 1

The molecular structure of (I), with the atom-labelling scheme. Displacement ellipsoids are drawn at the 40% probability level. C atoms are shown as small circles of arbitrary size and H atoms have been omitted for clarity.

the weak *trans* effect of the phenolate group. The longest bond on the N_3O_3 side is that to tertiary amine atom N1 [2.335 (3) Å]. This value is rather similar to those found in (II) and (III) [2.313 (2) and 2.279 (3) Å, respectively].

The coordination sphere of Mn2 is complemented by atoms N4 and N42 from the tertiary amine and pyridine group, and atom O50 from the terminal phenolate (hard side). The bond lengths around Mn^{III} (mean 2.041 Å) are quite similar to those found in (II) (mean 2.052 Å), and the longer axial bond lengths [Mn2–N42 = 2.278 (3) Å and Mn2–O62 = 2.129 (3) Å] are consistent with a Jahn–Teller distortion of this high-spin d^4 ion. The terminal Mn^{III}–O_{phenolate} bond [1.825 (3) Å] and Mn^{III}··Mn distance [3.466 (1) Å] are slightly shorter than those found in (II) [1.852 (2) and 3.497 Å, respectively], as expected, due to the effect caused by the *tert*-butyl substituents.

The Mn1–O1–Mn2 bridging angle of 116.8 (1)° falls within the range found for similarly coordinated mixed-valence manganese dimers with the structural [Mn^{III}Mn^{II}(μ -phenoxo)(μ -OAc)₂] unit. In (II), this angle is 116.6°, in [Mn₂(L-Im)(μ -OAc)₂]⁺ it is 116.8° [HL-Im is 2,6-bis[[(1-methylimidazol-2-yl)methyl]amino]methyl]-4-methylphenol; Buchanan *et al.*, 1988], in [Mn₂(bpmp)(μ -OAc)₂]⁺ it is 114.4° {Hbpmp is 2,6-bis[bis(2-pyridylmethyl)aminomethyl]-4-methylphenol; Diril *et al.*, 1989} and in [Mn₂(μ -L)(μ -OAc)₂(H₂O)]²⁺ it is 115.59° {HL is 2-[*N*-bis(2-pyridylmethyl)aminomethyl]-6-[*N*-(benzyl)(2-pyridylmethyl)aminomethyl]-4-methylphenol; Dubois *et al.*, 2003}.

Redox potentials are strongly dependent on the electronic character of the ligand substituent and on the asymmetry of the ligand. It is interesting to note that, despite the similarities of the averaged bond lengths and angles in the isostructural

complexes (I) and (II), the $E_{1/2}$ value of the redox couple [Mn^{II}Mn^{III}]/[Mn^{II}Mn^{II}] is cathodically shifted by 55 mV, a result which is consistent with the electron-donating effect of the *tert*-butyl groups and the slightly shorter Mn^{III}–O_{phenolate} bond length in complex (I), as described above. As reported by Miyasaka *et al.* (2003), the redox potentials can exhibit a linear correlation with the Hammett substituent constant σ_p .

In summary, a new unsymmetrical mixed-valence Mn^{II}–Mn^{III} complex has been structurally characterized and provides the possibility of studies of peroxide disproportionation and of correlating the redox potential and ligand field contribution to the rate and efficiency of this catalytic process.

Experimental

The ligand H₂Ldtb was prepared as follows. To a solution of 2-[bis(2-pyridylmethyl)aminomethyl]-6-[(2-pyridylmethyl)aminomethyl]-4-methylphenol (Greatti *et al.*, 2004) (3.4 g, 8 mmol) in dichloromethane, triethylamine (1.21 g, 12 mmol) and 4,6-di-*tert*-butyl-2-(chloromethyl)phenol (Sokolowski *et al.*, 1997) (3.02 g, 12 mmol) were added. The resulting mixture was allowed to react for 24 h while being stirred at room temperature. The product was extracted with aqueous NaHCO₃ solution (8 × 50 ml). The organic layers were dried over Na₂SO₄, the solvent was removed under reduced pressure and a pale-yellow solid was obtained (4.65 g, 7.2 mmol, yield 90%). ¹H NMR (CDCl₃): δ 8.54, 7.61, 7.53, 7.15, 6.97, 6.84 (16H, aromatic H), 3.92, 3.85, 3.84, 3.80 (*s*, 12H, CH₂), 2.23 (*s*, CH₃), 1.42, 1.25 (*s*, *tert*-butyl). Complex (I) was prepared by adding Mn(OAc)₂·4H₂O (1.0 mmol) and NaOAc (1.0 mmol) to a methanolic solution of the ligand H₂Ldtb (0.5 mmol) with stirring at 313 K for 20 min. The solution immediately turned dark red and then NaBPh₄ (0.5 mmol) was added. After slow evaporation of the solvent, dark-red crystals of (I) suitable for X-ray analysis were isolated (yield 82%).

Crystal data

[Mn₂(C₄₂H₄₉N₅O₂)(C₂H₃O₂)₂]-
(C₂₄H₂₀B)
M_r = 1203.04
Monoclinic, P₂₁/n
a = 16.492 (3) Å
b = 16.804 (3) Å
c = 24.519 (5) Å
β = 109.07 (3)°
V = 6422 (2) Å³
Z = 4

D_x = 1.244 Mg m⁻³
Mo Kα radiation
Cell parameters from 25
reflections
θ = 9.9–13.2°
μ = 0.45 mm⁻¹
T = 293 (2) K
Irregular block, dark red
0.47 × 0.40 × 0.13 mm

Data collection

Enraf–Nonius CAD-4
diffractometer
ω/2θ scans
Absorption correction: ψ scan
[(North *et al.*, 1968) and
PLATON (Spek, 2003)]
T_{min} = 0.829, T_{max} = 0.937
11638 measured reflections
11223 independent reflections

4980 reflections with I > 2σ(I)
R_{int} = 0.052
θ_{max} = 25.0°
h = 0 → 19
k = -19 → 0
l = -29 → 27
3 standard reflections
every 200 reflections
intensity decay: 1%

Refinement

Refinement on F²
R[F² > 2σ(F²)] = 0.052
wR(F²) = 0.127
S = 0.86
11223 reflections
784 parameters

H-atom parameters constrained
w = 1/[σ²(F_o²) + (0.058P)²]
where P = (F_o² + 2F_c²)/3
(Δ/σ)_{max} < 0.001
Δρ_{max} = 0.24 e Å⁻³
Δρ_{min} = -0.31 e Å⁻³

Table 1

Selected geometric parameters (Å, °).

Mn1—O61	2.067 (3)	Mn2—O50	1.823 (2)
Mn1—O71	2.139 (3)	Mn2—O1	1.905 (2)
Mn1—O1	2.161 (2)	Mn2—O72	1.984 (3)
Mn1—N32	2.237 (3)	Mn2—N4	2.118 (3)
Mn1—N22	2.262 (4)	Mn2—O62	2.129 (3)
Mn1—N1	2.335 (3)	Mn2—N42	2.278 (3)
O61—Mn1—O71	97.80 (13)	O50—Mn2—O72	86.59 (11)
O61—Mn1—O1	100.42 (11)	O1—Mn2—O72	92.36 (10)
O71—Mn1—O1	88.22 (10)	O50—Mn2—N4	88.71 (11)
O61—Mn1—N32	101.59 (13)	O1—Mn2—N4	91.88 (11)
O71—Mn1—N32	87.95 (11)	O72—Mn2—N4	167.14 (12)
O1—Mn1—N32	157.97 (11)	O50—Mn2—O62	92.03 (12)
O61—Mn1—N22	96.88 (14)	O1—Mn2—O62	90.15 (11)
O71—Mn1—N22	164.95 (13)	O72—Mn2—O62	97.88 (12)
O1—Mn1—N22	85.85 (10)	N4—Mn2—O62	94.24 (11)
N32—Mn1—N22	92.38 (12)	O50—Mn2—N42	91.52 (12)
O61—Mn1—N1	169.30 (13)	O1—Mn2—N42	86.42 (11)
O71—Mn1—N1	91.08 (11)	O72—Mn2—N42	89.94 (12)
O1—Mn1—N1	85.76 (10)	N4—Mn2—N42	78.22 (12)
N32—Mn1—N1	72.64 (12)	O62—Mn2—N42	171.59 (12)
N22—Mn1—N1	74.71 (13)	Mn2—O1—Mn1	116.74 (11)
O50—Mn2—O1	177.69 (12)		

The crystals of (I) grew from the mother solution as large prisms, but these diffracted poorly. Thus, the number of observed reflections in the *hkl* file is small (44%), giving rise to the consistency values R_{int} = 0.0518 and R_σ = 0.1572. One *tert*-butyl group is disordered and its terminal C atoms have two alternative positions, with occupancy

factors of 0.7 and 0.3. Some non-H atoms show abnormally high displacement parameters, but all these atoms were refined with anisotropic displacement parameters, with a positive definite thermal tensor. This gives high U_{eq}(max):U_{eq}(min) ratios for C and H atoms. H atoms were added in their calculated positions and included in the structure-factor calculations, with C—H distances of 0.93–0.96 Å and U_{iso}(H) = 1.2U_{eq}(C), or 1.5U_{eq}(C) for methyl atoms.

Data collection: CAD-4 EXPRESS (Enraf–Nonius, 1994); cell refinement: SET4 in CAD-4 EXPRESS; data reduction: HELENA (Spek, 1996); program(s) used to solve structure: SIR97 (Altomare *et al.*, 1999); program(s) used to refine structure: SHELXL97 (Sheldrick, 1997); molecular graphics: ORTEP-3 (Farrugia, 1997); software used to prepare material for publication: SHELXL97.

This work was supported by FINEP and CNPq.

Supplementary data for this paper are available from the IUCr electronic archives (Reference: TA1508). Services for accessing these data are described at the back of the journal.

References

- Altomare, A., Burla, M. C., Camalli, M., Cascarano, G., Giacovazzo, C., Guagliardi, A., Moliterni, A. G. G., Polidori, G. & Spagna, R. (1999). *J. Appl. Cryst.* **32**, 115–119.
- Antonyuk, S. V., Melik-Adamyanyan, W. R., Popov, A. N., Lamzin, V. S., Hempstead, P. D., Harrison, P. M., Artymiuk, P. J. & Barynin, V. V. (2000). *Crystallogr. Rep.* **45**, 111–122.
- Barynin, V. V., Hempstead, P. D., Vagin, A. A., Antonyuk, S. V., Melik-Adamyanyan, W. R., Lamzin, V. S., Harrison, P. M. & Artymiuk, P. J. (1997). *J. Inorg. Biochem.* **67**, 196.
- Buchanan, R. M., Oberhausen, K. J. & Richardson, J. F. (1988). *Inorg. Chem.* **27**, 971–973.
- Diril, H., Chang, H.-R., Nilges, M. J., Zhang, X., Potenza, J. A., Schugar, H. J., Isied, S. S. & Hendrickson, D. N. (1989). *J. Am. Chem. Soc.* **111**, 5102–5114.
- Dubois, L., Xiang, D.-F., Tan, X.-S., Pecaut, J., Jones, P., Baudron, S., Le Pape, L., Latour, J.-M., Baffert, C., Chardon-Noblat, S., Collomb, M.-N. & Deronzier, A. (2003). *Inorg. Chem.* **42**, 750–760.
- Enraf–Nonius (1994). CAD-4 EXPRESS. Version 5.1/1.2. Enraf–Nonius, Delft, The Netherlands.
- Farrugia, L. J. (1997). *J. Appl. Cryst.* **30**, 565.
- Greatti, A., de Brito, M. A., Bortoluzzi, A. D. & Ceccato, A. S. (2004). *J. Mol. Struct.* **688**, 185–190.
- Karsten, P., Neves A., Bortoluzzi, A. J., Lanznaster, M. & Drago, V. (2002). *Inorg. Chem.* **41**, 4624–4626.
- Karsten P., Neves A., Bortoluzzi, A. J., Strähle, J. & Maichle-Mössmer, C. (2002). *Inorg. Chem. Commun.* **5**, 434–438.
- Khangulov, S. V., Barynin, V. V., Voevodskaya, N. V. & Grebenko, A. I. (1990). *Biochim. Biophys. Acta Bioenergetics*, **1020**, 305–310.
- Miyasaka, H., Izawa, T., Sugiura, K. I. & Yamashita, M. (2003). *Inorg. Chem.* **42**, 7683–7690.
- North, A. C. T., Phillips, D. C. & Mathews, F. S. (1968). *Acta Cryst.* **A24**, 351–359.
- Sheldrick, G. M. (1997). SHELXL97. University of Göttingen, Germany.
- Sokolowski, A., Jochen, M., Weyhermuller, T., Schnepf, R., Hildebrandt, P., Hildebrandt, K., Bothe, E. & Wieghardt, K. (1997). *J. Am. Chem. Soc.* **119**, 8889–8900.
- Spek, A. L. (1996). HELENA. University of Utrecht, The Netherlands.
- Spek, A. L. (2003). *J. Appl. Cryst.* **36**, 7–13.
- Waldo, G. S. & Penner-Hahn, J. E. (1995). *Biochemistry*, **34**, 1507–1512.
- Wu, A. J., Penner-Hahn, J. E. & Pecoraro, V. L. (2004). *Chem. Rev.* **104**, 903–938.